

This is the author's final, peer-reviewed manuscript as accepted for publication. The publisher-formatted version may be available through the publisher's web site or your institution's library.

## An accurate and portable solid state neutron rem meter

T. M. Oakes, S. L. Bellinger, W. H. Miller, E. R. Myers, R. G. Fronk, B. W. Cooper, T. J. Sobering, P. R. Scott, P. Ugorowski, D. S. McGregor, J. K. Shultis, and A. N. Caruso

### How to cite this manuscript

If you make reference to this version of the manuscript, use the following information:

Oakes, T. M., Bellinger, S. L., Miller, W. H., Myers, E. R., Fronk, R. G., Cooper, B. W., ... Caruso, A. N. (2013). An accurate and portable solid state neutron rem meter. Retrieved from <http://krex.ksu.edu>

### Published Version Information

**Citation:** Oakes, T. M., Bellinger, S. L., Miller, W. H., Myers, E. R., Fronk, R. G., Cooper, B. W., ... Caruso, A. N. (2013). An accurate and portable solid state neutron rem meter. *Nuclear Instruments and Methods in Physics Research A*, 719, 6-12.

**Copyright:** © 2013 Elsevier B.V.

**Digital Object Identifier (DOI):** doi:10.1016/j.nima.2013.03.060

**Publisher's Link:** <http://www.sciencedirect.com/science/article/pii/S0168900213003707>

This item was retrieved from the K-State Research Exchange (K-REx), the institutional repository of Kansas State University. K-REx is available at <http://krex.ksu.edu>

# An Accurate and Portable Solid State Neutron Rem Meter

T.M. Oakes<sup>1</sup>, S.L. Bellinger<sup>2</sup>, W.H. Miller<sup>1,4</sup>, E.R. Myers<sup>3</sup>, R.G. Fronk<sup>2</sup>, B.W. Cooper<sup>2</sup>, T.J. Sobering<sup>5</sup>, P.R. Scott<sup>3</sup>, P. Ugorowski<sup>2</sup>, D.S. McGregor<sup>2</sup>, J.K. Shultis<sup>2</sup> and A.N. Caruso<sup>3\*</sup>

<sup>1</sup>Nuclear Science and Engineering Institute, University of Missouri – Columbia

<sup>2</sup>Department of Mechanical and Nuclear Engineering, Kansas State University

<sup>3</sup>Department of Physics, University of Missouri – Kansas City

<sup>4</sup>Missouri University Research Reactor, Columbia, MO

<sup>5</sup>Electronics Design Laboratory, Kansas State University

Keywords: neutron dosimeter, solid state neutron detector, spectrometer

## Abstract

Accurately resolving the ambient neutron dose equivalent spanning the thermal to 15 MeV energy range with a single configuration and lightweight instrument is desirable. This paper presents the design of a portable, high intrinsic efficiency, and accurate neutron rem meter whose energy-dependent response is electronically adjusted to a chosen neutron dose equivalent standard. The instrument may be classified as a moderating type neutron spectrometer, based on an adaptation to the classical Bonner sphere and position sensitive long counter, which, simultaneously counts thermalized neutrons by high thermal efficiency solid state neutron detectors. The use of multiple detectors and moderator arranged along an axis of symmetry (e.g., long axis of a cylinder) with known neutron-slowing properties allows for the construction of a linear combination of responses that approximate the ambient neutron dose equivalent. Variations on the detector configuration are investigated via Monte Carlo N-Particle simulations to minimize the total instrument mass while maintaining acceptable response accuracy - a dose error less than 15% for bare <sup>252</sup>Cf, bare AmBe, an epi-thermal and mixed monoenergetic sources is found at less than 4.5 kg moderator mass in all studied cases. A comparison of the energy dependent dose equivalent response and resultant energy dependent dose equivalent error of the present dosimeter to commercially-available portable rem meters and the prior art are presented. Finally, the present design is assessed by comparison of the simulated output resulting from applications of several known neutron sources and dose rates.

Submission: Nuclear Instruments and Methods in Physics Research A

Version: 25 FEB 2013

\*Corresponding Author: Anthony N. Caruso, [carusoan@umkc.edu](mailto:carusoan@umkc.edu), 816-235-2505

40 **1. Introduction**

41 The first wide-energy range instrument for measuring neutron dose equivalent was introduced in  
42 1962 by D.E. Hankins [1]. The Hankins moderating instrument, building on the ten-inch Bonner  
43 sphere response [2], was a paradigm shifting technology in neutron dose equivalent metrology in  
44 that the energy dependent dose equivalent [3-5] from thermal to ones-of-MeV could be  
45 approximated without directly measuring the neutron energy spectrum.

46

47 Since the mid-1960s, five classes of wide-energy range neutron dosimeters have emerged in an  
48 effort to improve: (1) the accuracy of measured quantities proportional to neutron energy; (2) the  
49 intrinsic detection efficiency; (3) the instrument mass; and/or (4) to extend the neutron energy  
50 range. These classes include: single or multiple detectors enclosed by single or multiple neutron  
51 interaction materials. In the first class, a combination of boron and/or cadmium, lead or tungsten,  
52 and high hydrogen concentration material (usually, high density polyethylene, or HDPE) are  
53 used as filters, spallation centers, and moderators to provide ever better response to the dose  
54 equivalent curve at up to ones-of-GeV incident neutron energy (e.g., Canberra's SNOOPY or  
55 Thermo's SWENDI-II) [6-12]. These instruments are known colloquially as the *Andersson-*  
56 *Braun* (AB) type. The downside of this approach is that the total mass is high (usually >10 kg)  
57 and the intrinsic detection efficiency is low (0.25% and 0.05% for the SWENDI-II and SNOOPY  
58 respectively, in response to bare  $^{252}\text{Cf}$ ). In the second case, multi-band detectors usually tune  
59 three or more detectors to the thermal, epithermal, and fast neutron spectrum ranges of the dose  
60 equivalent curve using filtering techniques but without extraneous moderator [13-18]. The  
61 implication is a lightweight dose equivalent meter (e.g., Ludlum's PRESCILA) but the average  
62 dose- and dose-rate error over the thermal to fast range is consequently the highest of the five

63 methods because of severe over or under response in the bands not covered. The third method  
64 employs many individual thermal neutron detectors in an HDPE or comparable moderating  
65 matrix to provide a depth dependent intensity of thermalized neutrons that yields both the highest  
66 efficiency and lowest average dose- and dose-rate-error of the above methods [19-27]. The  
67 shortfall of these instruments is their large moderating volume (usually a 30 cm diameter sphere)  
68 needed to accommodate tens-to-hundreds of individual detectors, rendering a non-portable  
69 device (>18 kg with electronics). The fourth method utilizes a single position sensitive detector  
70 enclosed by moderator and filter materials as an improvement to the classical long counter [28-  
71 30]. Although simple, this detection scheme suffers from large moderating volumes and low  
72 intrinsic efficiency due to high neutron absorption in the moderator and/or scattering of neutrons  
73 outside the detector volume. There are only a few examples of the fifth class which utilize a  
74 combination of elements from the first three [31-35]. Like the second class, these dosimeter  
75 schemes use a superposition of responses to better approximate the dose equivalent curve, but  
76 they incorporate an important improvement in that the overlapping energy response bands are  
77 continuous. This provides for a much better dose equivalent match, even up to ones-of-GeV,  
78 than that available commercially. The downside is, again, the large total volume and low  
79 intrinsic efficiency. Neither the third, fourth, nor fifth device classes have been adopted for  
80 commercial production.

81  
82 Due to their minimum size requirements, the continued use of gaseous- and scintillator-based  
83 thermal neutron detectors in wide-energy, moderating-type neutron dosimeters perpetuates an  
84 intrinsic tradeoff between dose error (closest match to the dose equivalent curve), volume of  
85 moderator needed, and total detection efficiency (or time/fluence needed to attain reasonable

86 statistics). For the moderating-type classes given above, these tradeoffs can be lessened via a  
87 cross-over to solid state methods of neutron detection that allow for a reduced perturbation to the  
88 neutron slowing down process (i.e. increased spatial detection resolution) as well as  
89 enhancements to intrinsic efficiency. The reduced perturbation stems from the ability to fabricate  
90 devices (p-n junctions) nearly wafer thin (<500  $\mu\text{m}$ ) while retaining high intrinsic efficiency. The  
91 high intrinsic efficiency is derived from both the high thermal detection efficiency capabilities  
92 (described elsewhere [37]) as well as the detector-moderator geometry (i.e., minimizing neutron  
93 absorption in the moderator). The work reported here describes a significantly improved method  
94 for measuring the ambient neutron dose equivalent through a combination of superposed  
95 detectors and electronic response matching to the dose equivalent standard [38]. The result is a  
96 portable instrument that is adjustable to any dose equivalent quantity, but still retains high  
97 intrinsic efficiency, and low dose equivalent error for neutrons with energy less than 15 MeV.

98

## 99 **2. Design Philosophy**

100 The operational quantity devised by the International Commission on Radiation Units and  
101 Measurement (ICRU) for operational radiation field measurements is the ambient dose  
102 equivalent,  $H^*(10)$ , which represents the dose equivalent at a point of interest in a radiation field  
103 which would be generated at a 10 mm depth in a superimposed tissue-equivalent sphere [39]. For  
104 the case of mono-energetic neutrons at energy  $E$ , the ambient dose equivalent can be determined  
105 by

106

$$H^*(10) = \Phi h_{cc,E} \quad (1)$$

107

108 where  $\Phi$  is the mono-energetic neutron fluence and  $h_{cc,E}$  is a neutron dose-equivalent conversion  
109 value specific to the energy of the incident neutrons that accounts for both the quantity of energy  
110 absorption and the corresponding relative biological effects (Fig. 1a). Realistic dosimetric  
111 applications, however, deal primarily with neutron fields that occupy one or several decades of  
112 energy such that is necessary to generalize our expression for the ambient dose equivalent as  
113

$$H^*(10) = \int_0^{\infty} \Phi(E) h_{cc}(E) dE \quad (2)$$

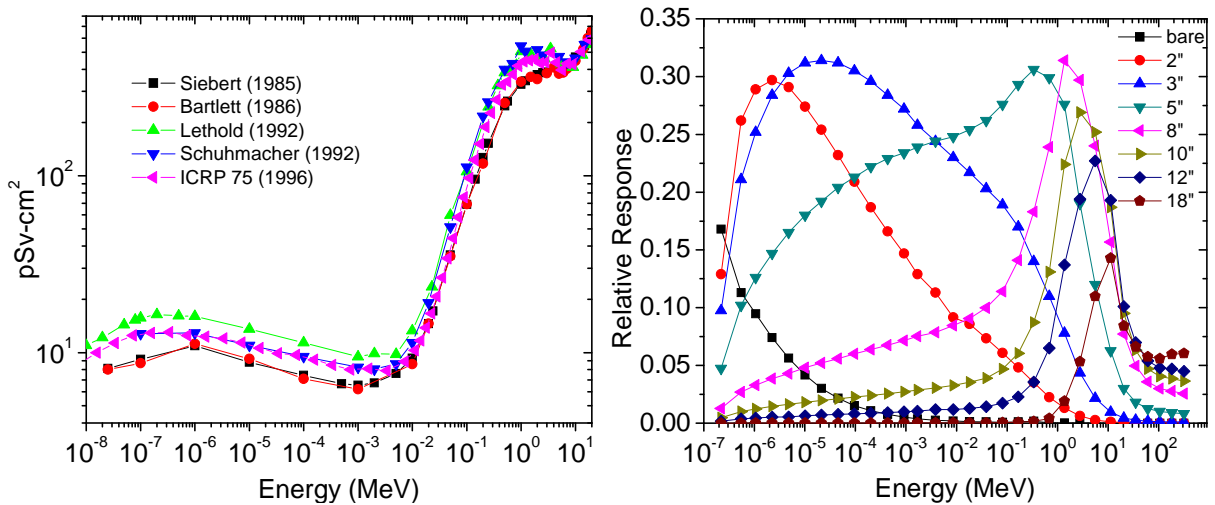
114  
115 where  $\Phi(E)$  contains the neutron energy characteristics (generally unknown) and  $h_{cc}(E)$  is a  
116 fluence-to-ambient dose equivalent conversion function. Note that  $h_{cc}(E)$  is a highly nonlinear  
117 function in energy wherein relatively low dose equivalent per unit neutron fluence ( $\sim 10$  pSv-  
118  $\text{cm}^2$ ) is observed at energies below 10 keV followed by a nearly two order-of-magnitude increase  
119 ( $\sim 600$  pSv- $\text{cm}^2$ ) between 10 keV and 1 MeV as demonstrated in Figure 1a. This work will focus  
120 on  $h_{cc}(E)$  data presented by the International Committee on Radiological Protection (ICRP) in  
121 publication 74 [4].

122  
123 Known neutron energy intensity as a function of axial or radial depth into a moderator (Figure  
124 1b) permits the application of a Fredholm integral equation of the first kind as

$$N(k) = \int_0^{\infty} R(E, k) \Phi(E) dE \quad (3)$$

126

127 where  $N(k)$  is the pulse height for energy bin  $k$  with a known response matrix  $R$ . Such analyses  
 128 are commonly performed on Bonner sphere systems [2], utilizing multiple diameter spherical  
 129 moderators to provide different levels of thermalization for incident neutrons – each individual  
 130 moderator configuration corresponding to an exclusive, energy-dependent thermalization  
 131 efficiency curve that populates the  $R(E, k)$  term (Fig. 1b). Neutrons that thermalize as they reach  
 132 the instrument’s center can be detected and used to populate  $N(k)$ , thereby transforming  
 133 Equation (3) into an ill-posed, under-determined inversion problem [40] requiring a spectral  
 134 unfolding technique to determine  $\Phi(E)$ . Solution(s) obtained in this manner are not unique and  
 135 do not depend continuously on the data such that a more reliable, less computationally expensive  
 136 method is desirable for real-time dosimetric applications.



137  
 138 **Fig. 1.** (a) Various incarnations of the ambient dose equivalent conversion curve (■ Siebert, ●  
 139 Bartlett, ▲ Lethold, ▼ Schuhmacher, ◀ ICRP 74; adapted from [4, 41-45]); (b) response curves  
 140 from several Bonner sphere configurations.

141  
 142 The need for a portable, real-time neutron dose-equivalent meter was first addressed by Hankins  
 143 [1] in the form of a single thermal neutron detector surrounded by moderating material –

144 essentially an adaptation of Bonner's spectrometer utilizing a single, fixed configuration. This  
145 "rem meter" exhibits a measurement response

146

$$M = \int_0^{\infty} C\Phi(E) d_{cc}(E)dE \quad (4)$$

147

148 where  $C$  is a calibration constant and  $d_{cc}(E)$  is the energy-dependent detector response function.

149 Note the similarity in form between equations (2) and (4). Assuming that the neutron fields are

150 identical, it has been shown that matching the shape of a neutron detector's energy response

151 curve to the fluence-to-ambient dose equivalent conversion function provides an approximate

152 means of determining the neutron dose equivalent without the need to resolve the actual incident

153 energies [6]. A brief comparison of Figure 1a and 1b enables the reader to infer the similarity in

154 shape between the response of the 10 to 18" Bonner spheres and the ambient dose equivalent

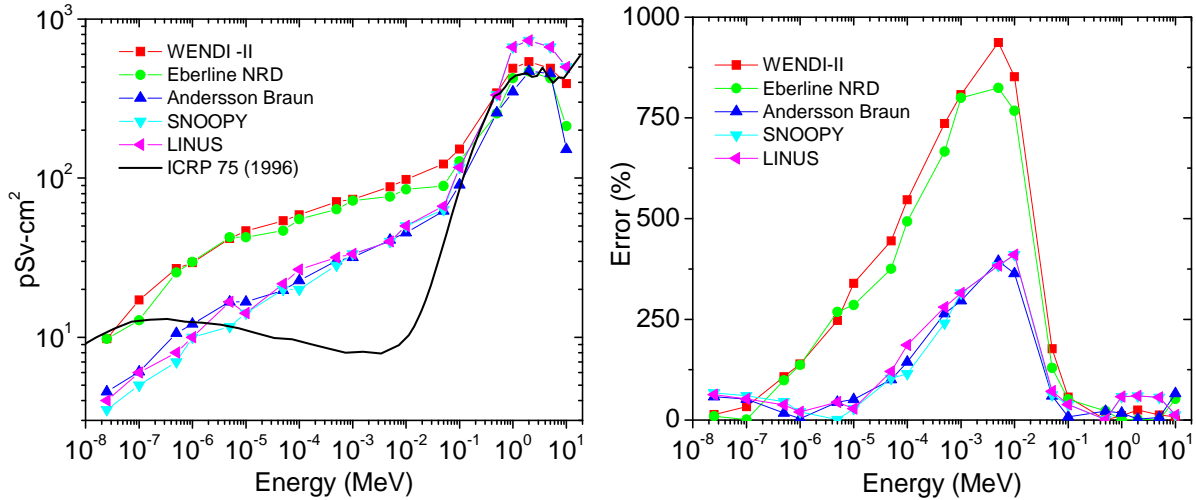
155 coefficients up to ~8 MeV. The resulting Andersson-Braun design (1963) and its variants (Fig. 2)

156 have been used to formulate several real-time devices including the SNOOPY (1964), LINUS

157 (1975), and WENDI-II (1995) [6-12].

158





159

160 **Fig. 2.** (a) Calculated neutron-dose-equivalent energy-response for several neutron  
 161 detection/dosimetry models (■ WENDI-II, ● Eberline NRD, ▲ Andersson Braun, ▼ SNOOPY,  
 162 ◀ LINUS, --- ICRP 74; adapted from [4, 6-12]); (b) and their associated error with respect to  
 163 ICRP 74 fluence-to-ambient dose equivalent conversion values.

164

165 Each of the detector responses shown in Figure 2 exhibit average errors ranging from 20 to 50  
 166 percent in the thermal and fast regions with considerable error present in the epithermal energy  
 167 range (i.e., > 950% of  $h_{cc}(E)$  for the WENDI-II [4, 41-45]). One may conclude that the accuracy  
 168 of such matching schemes is inherently limited by the use of a single detector and moderator  
 169 configuration.

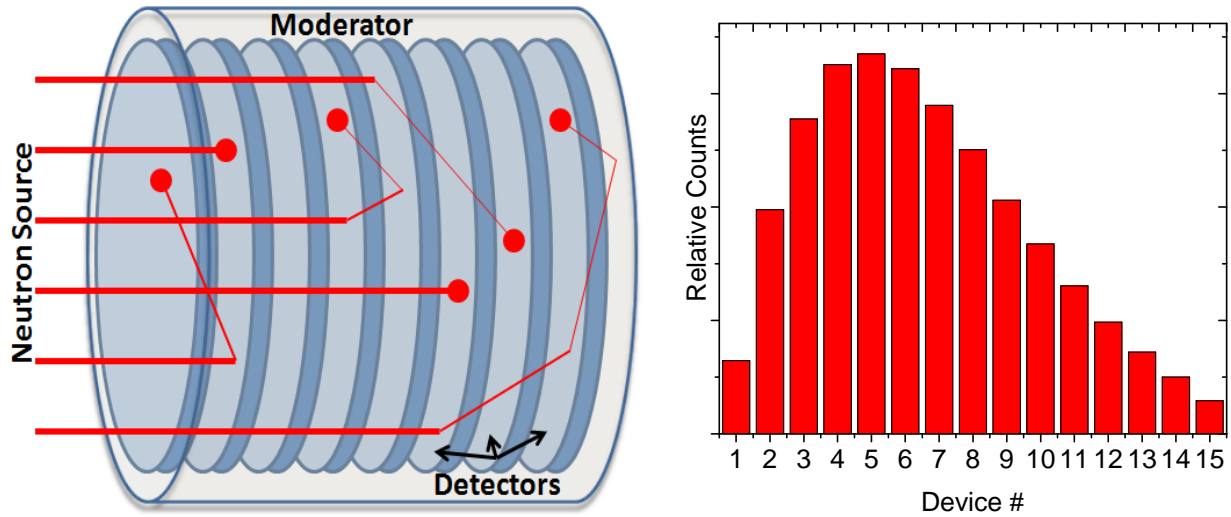
170

171 In order to accurately match the non-linear shape of the ambient dose equivalent conversion  
 172 curve (or any future revisions that may result in its modification – Figure 1a) it is necessary – in  
 173 comparison with Bonner’s work and as an improvement on the position sensitive long counter  
 174 [46] – to resolve (within  $\sim 1 \text{ cm}^3$ ) where incident neutrons reach thermal energy in a moderating  
 175 volume along one or more geometric coordinate axes. For the case of free neutrons travelling in

176 parallel, this task can be accomplished by stacking high thermal efficiency solid state detectors  
177 (or comparable thin high thermal efficiency detectors), into an axially symmetric moderator  
178 geometry, like that of a right cylinder as shown by Figure 3a. “Thin” detectors are important as  
179 they reduce the neutron scattering perturbation and reduce the total instrument volume. The ~1  
180 cm<sup>3</sup> volume resolution recommendation is chosen as a volume that will yield fine enough  
181 scattering length determination to accurately quantify the neutron dose over many  
182 logarithmic energy intervals. The volumetric or three-dimensional resolution comes from  
183 stacking (1-D) pixelated (2-D) detectors. By doing so, not only can a real time response be  
184 generated, but the conversion curve can also be adjusted electronically. Note, a non-pixelated  
185 version, with stacking, that provides only 1-D resolution along the axial coordinate of a cylinder  
186 is also possible. Further, it is possible to replace the solid-state detectors, as long as the replacing  
187 detector(s) is/are comparably low volume relative to the overall volume and has (or can be  
188 summed to provide) at least one-dimensional position sensitivity. In the case of the instrument  
189 described here, it is assumed that the neutrons are parallel and incident on the front face of the  
190 right cylinder as shown in Figure 3a. In applications with significant scattering, the instrument  
191 would be covered by a material that absorbs thermal neutrons, such as cadmium or a boron  
192 compound, and the absorbing layer covered with moderator to avoid detecting epithermal and  
193 fast neutrons from the sides or back (i.e. a camera geometry). Conversely, if there were very few  
194 neutrons and they were incident from all directions, a spherical geometry with radial dependence  
195 would be optimal. For the instrument described henceforth, the discussion is focused on the 1-D  
196 version (i.e., axial dependence) of the cylindrical geometry wherein  $n$  neutron detectors are  
197 stacked at 1.0 cm center-to-center spacing and oriented to maintain axial symmetry within a  
198 hydrogenous moderator of comparable radius (Figures 3a and 4a). Moderator length (axial

199 dimension) is chosen in consideration of the scattering length needed to accurately resolve the  
200 dose of 15 MeV neutrons (i.e. ~15.0 cm).

201



202

203 **Fig. 3.** (a) Adaptation of the Bonner Sphere system into a cylindrical symmetry with solid state  
204 thermal neutron detectors allowing for simultaneous detector response as a function of the axial  
205 dimension; (b) histogram tallies of measured counts (point of thermalization) from bare  $^{252}\text{Cf}$   
206 [48] as a function of axial position into the moderator.

207

208 The 1-D axial binning scheme is presented in the form of a histogram in Figure 3b, unique to the  
209 energy and intensity of the incident neutron source (unmoderated  $^{252}\text{Cf}$  in this case). The  
210 thickness/volume of a solid-state detector is defined by the semiconductor element and any  
211 necessary electronics that must be in the neutron path (e.g., preamplifiers, fiberglass boards,  
212 etc.). One means of meeting the needed specifications for thermal efficiency, large area and low  
213 volume (i.e., thin) are the indirect-conversion, solid state neutron detectors developed at Kansas  
214 State University [37]. These microstructured neutron detectors (MSNDs) are comprised of  
215 silicon micro-structural trenches, doped and contacted to enable a p-n junction, and backfilled

216 with enriched  ${}^6\text{LiF}$  powder. The microstructure dimensions and lower level discriminator settings  
217 have been optimized for the  ${}^6\text{Li}$  primary reaction products mean free paths to yield devices with  
218 22% thermal neutron detection efficiency. Because standard VLSI methods are used to process  
219 the MSNDs, device radii in excess of 10 cm – built either from a single 200 mm wafer or from  
220 the superposition of wafer slices from 125 mm wafers – are possible and explored as an upper  
221 bound in the calculations described below.

222

223 The minimal perturbation of each detector to the moderation process, combined with the high  
224 thermal efficiency of each solid-state element, permits the investigation of an individual device's  
225 output with respect to the corresponding degree of observed moderator penetration. Energy  
226 dependence considerations allow for the delivery of distinct efficiency vs. energy curves as a  
227 function of moderator thickness that closely resembles the acquisition from collections of Bonner  
228 sphere configurations (Fig. 1a) – but in real time and without the significant non-detectable  
229 absorption that occurs in the Bonner Sphere and related instruments. The availability of  $n$   
230 simultaneous measurements from  $n$  detectors with unique, Bonner-like response functions  
231 permits revision of its rem meter's dose response curve to

232

$$M = \int_0^{\infty} \Phi(E) f(d_{cc,1}(E), \dots, d_{cc,n}(E)) dE \quad (5)$$

233

234 where the single detector response curve of a conventional rem meter is replaced by some  
235 function,  $f$ , of multiple response curves,  $d_{cc,1}(E) - d_{cc,n}(E)$ , to permit more accurate matching to  
236  $h_{cc}(E)$ . It is proposed that a linear combination of the individual Bonner-like response functions

237 can be used to force the rem meter's overall response function to mimic the shape of the provided  
 238 fluence-to-ambient dose equivalent conversion function such that

239

$$f(d_{cc,1}(E), \dots, d_{cc,n}(E)) = h_{cc}(E) = \sum_{i=1}^n g_i d_{cc,i}(E) \quad (6)$$

240

241 where  $g_i$  is the gain corresponding to the  $i_{th}$  detector's response function. It is this gain that  
 242 allows for the electronic matching to any dose equivalent curve. A collection of measurements  
 243 from  $m$  mono-energetic sources spanning the pertinent energy range are required to populate an  
 244  $m$  by  $n$  matrix,  $B$ , where the corresponding  $h_{cc}(E)$  values populate a  $m$  by 1 column matrix,  $y$ .  
 245 The discrete Fredholm equation is then expressed as

246

$$y_{(m,1)} = B_{(m,n)} G_{(n,1)} \quad (7)$$

247

248 where  $G$  is the gain matrix containing  $n$  optimal multiplier values ( $g_1-g_n$ ). Assuming an over-  
 249 determined system, identification of the optimal gain values is now accomplished by  
 250 minimization of a "cost" function, selected for this case to be the sum of the square of the  
 251 residuals

252

$$J = [y_{(m,1)} - B_{(m,n)} G_{(n,1)}]^T R_{(m,m)}^{-1} [y_{(m,1)} - B_{(m,n)} G_{(n,1)}] \quad (8)$$

253

254 where  $R$  is a diagonal matrix populated by the desired weights, for this case the inverse square  
 255 values of  $y$  [47]. Assuming  $B$  is invertible

256

$$G_{(n,1)} = [B_{(n,m)}^T R_{(m,m)}^{-1} B_{(m,n)}]^{-1} B_{(n,m)}^T R_{(m,m)}^{-1} Y_{(m,1)} \quad (9)$$

257

258 Once the gain values are determined, the ambient dose equivalent due to a cumulative detector  
259 response (i.e.  $n$  detectors) can be determined from a series of backward substitutions as

260

$$H^*(10) = \sum_{i=1}^n g_i M_i \text{ (}\mu\text{Sv)} \quad (10)$$

261

262 where  $M_i$  denotes the number of counts on the  $i^{\text{th}}$  detector, or

263

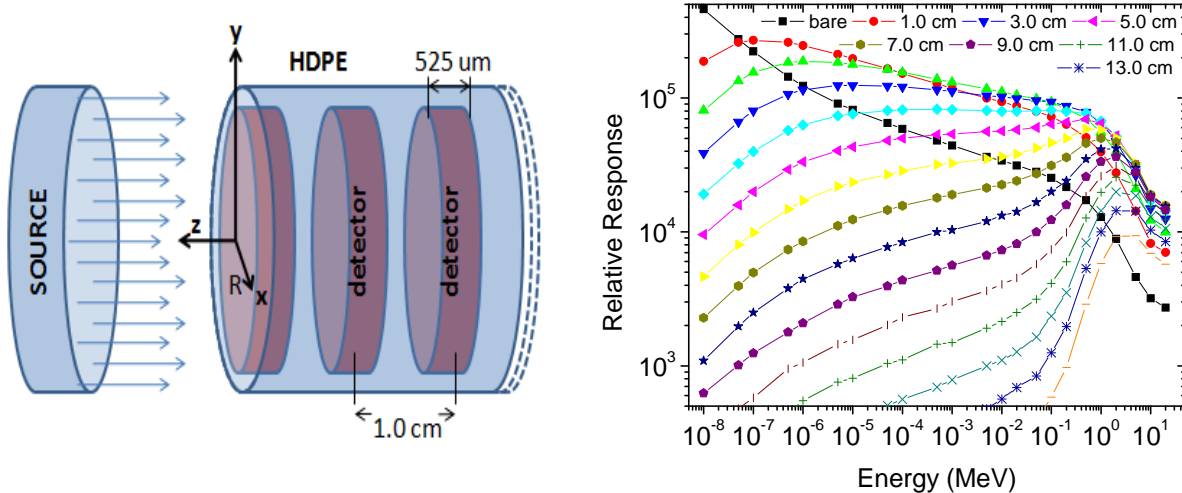
$$M_i = \int_0^{\infty} \Phi(E) d_{cc,i}(E) dE \quad (11)$$

264

### 265 3. Computational Modeling

266 Instrument studies were performed using the Monte Carlo N-Particle code (MCNP), specifically  
267 MCNPX 2.6.0 for charged particle transport. All experiments conducted in the current study  
268 utilize a similar, high-density polyethylene moderated model (Fig. 4a) with simulations driven by  
269 a planar source of 5000 neutrons per  $\text{cm}^2$  – in all cases the source radius is set equal to the  
270 detector/moderator radius. Neutron detectors are modeled as 525  $\mu\text{m}$ -thick cylinders of natural  
271 isotopic abundance silicon containing homogeneously interspersed quantities of neutron-  
272 sensitive material sufficient enough to yield 22% thermal detection efficiency, commensurate  
273 with the efficiency obtained with the  $^6\text{LiF}$  solid state detectors developed at Kansas State

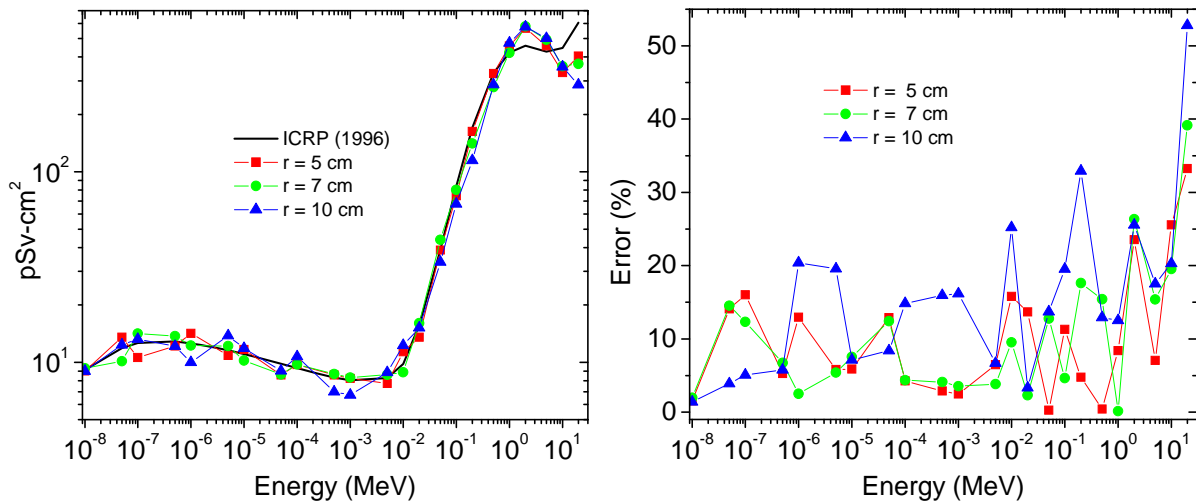
274 University [37]. Alpha production in each transduction cell is accounted via series of f4 tallies  
 275 where a one-to-one ratio exists between realized alpha particles and successfully detected  
 276 neutrons per the cell material definition. Three sets of primary simulations are conducted on a  
 277 generalized MCNPX model (Fig. 4a) with  $L = 15.0$  cm for detector radii of 5.0, 7.0, and 10.0 cm,  
 278 the latter combination corresponding to a maximum desired moderator mass of 4.5 kg. Each set  
 279 features a collection of 23 different mono-energetic neutron sources spaced logarithmically  
 280 between  $10^{-8}$  and 15 MeV with the results compiled into output histograms (one per simulation;  
 281 see Figure 3b for an example).



282  
 283 **Fig. 4.** (a) Generalized MCNPX model schematic for the solid state neutron spectrometer  
 284 reported here; (b) detector position specific response curves for the  $r = 10.0$  cm,  $L = 15.0$  cm  
 285 configuration.

286  
 287 Higher kinetic energy neutrons exhibit larger total path lengths between scattering interactions  
 288 needed to reach thermal energy, and are therefore capable of further axial penetrations into the  
 289 detector. This phenomenon yields count distributions (intensity as a function of axial position)  
 290 that feature markedly different uni-modal shapes as a function of energy. Tabulation of the

291 histogram collections permits presentation of the individual device efficiencies as a function of  
 292 neutron energy (Fig. 4b) that closely resemble the outputs of different Bonner sphere  
 293 configurations. Note that while the shape remains consistent between the different models, the  
 294 calculated values appear higher in all cases for larger volume detectors (10.0 cm > 7.0 cm > 5.0  
 295 cm) likely due to the subsequent increase in the relative number of probable scattering reactions  
 296 (i.e. intrinsic efficiency).  
 297



298  
 299 **Fig. 5.** Response (a) and error (b) of the instrument reported here for  $r = 5$  (■), 7 (●), 10 (▲) cm  
 300 and  $L = 15$  cm. The instrument response in (a) is compared to ICRP 74 fluence-to-ambient dose  
 301 equivalent conversion values.

302  
 303 Equations (6) – (10) are used in conjunction with the data acquired from each simulation set to  
 304 match the detector response function to the reference  $h_{cc}(E)$  curve (Fig. 5) where  $n = 15$  and  $m =$   
 305 23 (15 devices and 23 appropriately spaced mono-energetic simulations). As shown in Figure 5a,  
 306 each of the dosimeter radii exhibit excellent tracking of the reference  $h_{cc}(E)$  curve in the range  
 307 of thermal to 20 MeV. The average errors over the entire energy span measure 10.2, 10.5, and



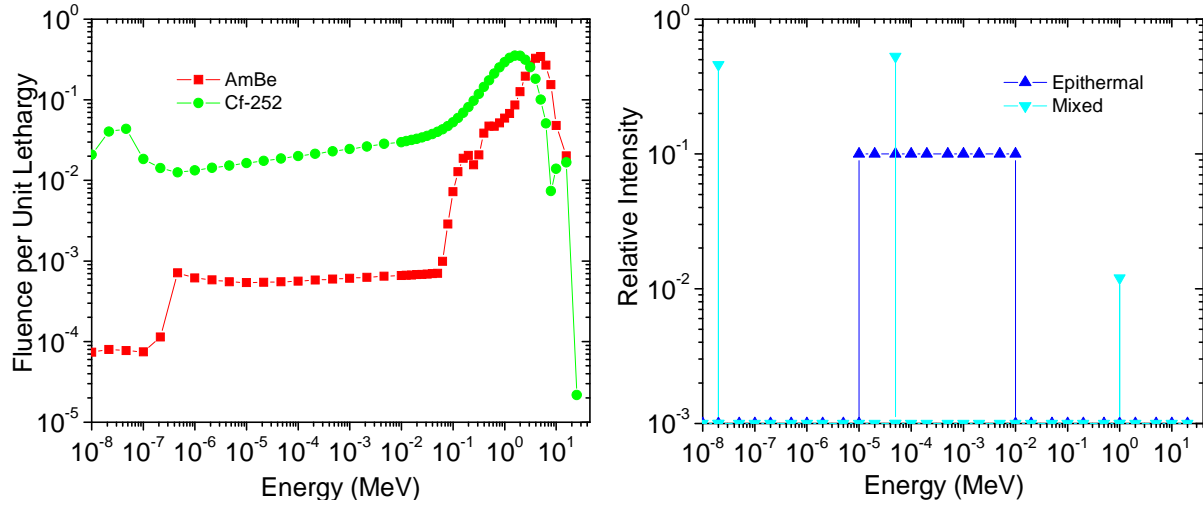
308 15.7 percent, respectively, with the absolute maximums observed between 15 and 20 MeV for all  
309 cases. These errors are significantly less than those of conventional rem meters displayed in  
310 Figure 2. In addition, the three proposed dosimeters evaluated here have moderator masses of  
311 only 1.1, 2.3, or 4.5 kg, depending on the radius utilized. In environments where scattered  
312 neutrons may impinge on the side or back of the instrument, the concentric cadmium wrapping  
313 and moderator (assuming ~3.0 cm thickness to appropriately thermalize most epithermal  
314 neutrons prior to passage through the cadmium layer) will add 1.7, 2.2 or 3.0 kg to the total  
315 instrument mass.

316

#### 317 **4. Model Validation and Discussion**

318 Validation of the computed ambient dose equivalent is accomplished through superposition of  
319 data sets collected from the 23 monoenergetic neutron simulations in section 3 to emulate four  
320 different neutron energy distributions: the first two constructed from the neutron spectra arising  
321 from the AmBe and <sup>252</sup>Cf sources (Fig. 6a [48]), the third from an unrealistic, entirely epithermal  
322 energy range, and the fourth from equal dose contributions of thermal, epithermal, and fast  
323 neutrons (Fig. 6b). The individual contributions from each simulation histogram/energy are  
324 modified to deliver a net dose of 10 μSv (1.0 mrem).

325



326

327 **Fig. 6.** (a) AmBe (■) and <sup>252</sup>Cf (●) source distributions [48]; (b) epithermal (▲) and mixed  
 328 monoenergetic (▼) source distributions.

329

330 The histogram data provided by each simulation output is used in conjunction with equation (10)  
 331 to estimate the ambient dose equivalent (Table 1). All of the models/estimates accurately account  
 332 for the delivered equivalent dose with all observed errors less than 15% for all cases (energy and  
 333 radii).

334

<i>Model/Source</i>	<b>AmBe (%)</b>	<sup>252</sup> <b>Cf (%)</b>	<b>Epithermal (%)</b>	<b>Mixed Mono (%)</b>
<b>R = 5.0 cm</b>	7.5	11.7	2.2	0.1
<b>R = 7.0 cm</b>	11.3	8.8	4.0	0.9
<b>R = 10.0 cm</b>	13.3	12.0	1.0	0.9

335 **Table 1:** Error in estimation of reference dose equivalent for neutron source distributions.

336

337 Note that most of this error is observed in the AmBe and  $^{252}\text{Cf}$  spectra and may be attributed to  
338 the fact that the majority of their respective dose contributions are derived from higher energy  
339 neutrons where the greatest disparity between  $h_{cc}(E)$  and instrument response is observed.  
340 Conversely, the doses delivered by epithermal and mixed mono-energetic neutron sources  
341 exhibit measurement errors less than 4% and speak directly to the accurate response-matching at  
342 energies below 1.0 MeV. Further enhancement to response-matching is likely attainable via  
343 design optimization (i.e. different length, radius, detector spacing, etc.) in conjunction with  
344 subsequent improvements to equation (6) (i.e. perhaps a more complicated function of the  
345 different response curves). Further, it is important to note that the current form of equation (6)  
346 permits both positive and negative multipliers which, with poor counting statistics, could lead to  
347 erroneous dose estimates. Although poor counting statistics are mitigated by the high neutron  
348 efficiency of this device, this effect will be addressed in future work.

349

350 In addition to size, mass, and energy-response characteristics, a rem meter's measurement  
351 sensitivity and/or intrinsic efficiency must also be considered when evaluating its overall  
352 performance. Canberra's NP2 SNOOPY – an 11.8 kg instrument commonly used for dosimetric  
353 surveys of reactor spectra – features a lateral sensitivity of  $\sim 10.0$  counts/minute per  $\mu\text{Sv}/\text{hour}$   
354 referenced to  $^{252}\text{Cf}$ . Assuming a total side-irradiation (24.38 cm by 40.64 cm) and 380 pSv-cm<sup>2</sup>  
355 average dose-equivalent per unit-neutron-fluence [48], this translates to 0.05% intrinsic  
356 efficiency. Despite errors upward of 400% in the epithermal energy region, the SNOOPY  
357 reportedly maintains 10% uncertainty with respect to reference dosimetric values (likely due to  
358 the generally mid-to-high-range energy spectra to which it is intended to encounter); however, as

359 many real world neutron fields comprise a significant scattering fraction, accurately resolving the  
360 epithermal neutron dose equivalent cannot be ignored.

361  
362 Thermo's WENDI-II incorporates the addition of spallation material (i.e. lead) that extends its  
363 energy range upwards of 5.0 GeV for monitoring neutron fields resulting from high-energy  
364 accelerators and/or cosmic interactions. The spallation centers consequently increases the total  
365 mass to 13.2 kg and increases the epithermal error above 900%. It too maintains a 10%  
366 uncertainty to unmoderated spontaneous-fission- or  $\alpha$ ,n-spectrum-type doses – most likely due to  
367 its accurate matching of the dose-equivalent curve at energies greater than 1.0 MeV – and  
368 exhibits a lateral sensitivity approximately five times greater than that of the SNOOPY (45.7  
369 counts/minute per  $\mu$ Sv/hour). Given the similar dimensions (22.86 cm by 33.67 cm) between the  
370 two devices, this increase in measurement sensitivity directly corresponds to a five-fold increase  
371 in observed intrinsic efficiency to 0.25%.

372  
373 In contrast to conventional neutron dose-equivalent survey technology, the instrument reported  
374 here permits dose-equivalent measurements in the energy range of thermal to 20.0 MeV within  
375 15% accuracy over the total range with less than half of the required mass. All three simulated  
376 systems exhibit intrinsic efficiencies to bare  $^{252}\text{Cf}$  of 10.25%, 18.89%, and 27.70% (for  $r = 5, 7,$   
377 and 10 cm, respectively) and measurement sensitivities in terms of raw count data of 353, 6,750,  
378 and 13,780 counts/minute per  $\mu$ Sv/hour (for  $r = 5, 7,$  and 10 cm, respectively). This significant  
379 increase in instrument sensitivity/intrinsic efficiency related to the SNOOPY or WENDI-II is  
380 based on the presence of high thermal efficiency detectors distributed 1 cm along the  
381 thermalization path which permit detection of neutrons that are otherwise lost to capture in

382 traditional instruments with a 12 cm moderator radius and single central detector. In  
383 concurrence, is important to note that the sensitivities and intrinsic efficiencies of the system  
384 described here, solely associated with the deepest detectors, are comparable with those of the  
385 SNOOPY and WENDI-II systems (i.e., ~0.25%).

386

## 387 **5. Summary and Future**

388 A new type of portable neutron rem meter is introduced based on the concept of a solid state  
389 neutron spectrometer. The instrument design and algorithm developed are motivated by the high  
390 error encountered with commercially available wide-energy range neutron dose equivalent  
391 instruments. The device utilizes real-time sampling of thermalized neutrons by multiple weakly  
392 perturbing and high thermal efficiency solid-state neutron detectors to provide simultaneous  
393 access to a number of Bonner-like response curves. A linear combination of the measurement  
394 signals permits excellent matching of the energy-dependent ambient dose equivalent coefficients  
395 with average errors less than 15%. Validation of the measured ambient equivalent neutron dose  
396 is accomplished using simulation-compiled AmBe,  $^{252}\text{Cf}$ , epithermal, and mixed mono-energetic  
397 spectra to yield absolute errors less than 15% for all cases. These investigations have yet to  
398 consider the propagation of counting statistics on individual detectors to the resulting dose  
399 prediction that will be needed to confirm dosimetry accuracy for low flux neutron dose fields  
400 and/or short counting times in the 15 second range typically associated with practical neutron  
401 dose survey meter applications.

402

## 403 **Acknowledgements**

404 The authors acknowledge partial support of this work by the Office of Naval Research under  
405 award No. N00014-11-1-0157. ANC wishes to thank Noel Guardala for helpful discussions in  
406 originating this work.

## 407 **References**

- 408
- 409 [1] Dale E. Hankins, Report LA-2717, Los Alamos Scientific Laboratory, Los Alamos  
410 (1962).
- 411
- 412 [2] R.L. Bramblett, R.J. Ewing and T.W. Bonner, *Nucl. Instrum. Methods* **9** (1960) 1.  
413
- 414 [3] ICRP, 2007. The 2007 Recommendations of the International Commission on  
415 Radiological Protection. *ICRP Publication* **103**. *Ann. ICRP* **37** (2-4).  
416
- 417 [4] ICRP, *Conversion Coefficients for Use in Radiological Protection against External*  
418 *Radiation*, Publication 74, International Commission on Radiological Protection, *Annals*  
419 *of the ICRP*, **26**, No. 3/4, Pergamon Press, Oxford, 1996.  
420
- 421 [5] J.C. McDonald, B.R.L. Siebert, W.G. Alberts, *Nuc. Inst. Meth. Phys. Res. A* **476** (2002)  
422 347.  
423
- 424 [6] Richard H. Olsher, Hsiao-Hua Hsu, Anthony Beverding, Jeffrey H. Kleck, William H.  
425 Casson, Dinnis G. Vasilik, Robert T. Devine, *Health Physics* **79** (2000) 170.  
426
- 427 [7] V. Mares, A.V. Sannikov, H. Schraube, *Nuc. Inst. Meth. Phys. Res. A* **476** (2002) 341.  
428
- 429 [8] C. Birattari, A. Ferrari, C. Nuccetelli, M. Pelliccioni, M. Silari, *Nuc. Inst. Meth. Phys.*  
430 *Res. A* **297** (1990) 250.  
431
- 432 [9] J.M. Brushwood, P.A. Beeley, N.M. Spyrou, *Nuc. Inst. Meth. Phys. Res. A* **476** (2002)  
433 304.  
434
- 435 [10] Chris Benson, Malcolm J. Joyce, Barry O-Connell, Jon Silvie, *IEEE Trans. Nuc. Sci.* **47**  
436 (2000) 2417.  
437
- 438 [11] M. Cosack, H. Lesiecki, *Rad. Prot. Dos.* **10** (1985) 111.  
439
- 440 [12] J.W. Leake, *Nuc. Inst. Meth.* **45** (1966) 151.  
441
- 442 [13] J.A. Weaver, M.J. Joyce, A.J. Peyton, J. Roskell, M.J. Armishaw, *Rev. Sci. Inst.* **72**  
443 (2001) 2043.  
444
- 445 [14] J.A. Weaver, M.J. Joyce, A.J. Peyton, J. Roskell, *Nuc. Inst. Meth. Phys. Res. A* **476**  
446 (2002) 143.

- 447  
448 [15] A.M. Williams, N.M. Spyrou, J.M. Brushwood, P.A. Beeley, *Nuc. Inst. Meth. Phys. Res.*  
449 *A* **476** (2002) 149.  
450  
451 [16] Gordon K. Riel, *Lightweight Neutron Remmeter*, United States Patent No. 6,930,311  
452 (2005).  
453  
454 [17] R. Olsher, D. Seagraves, S. Eisele, C. Bjork, W. Martinez, L. Romero, M. Mallett, M.  
455 Duran. C. Hurlbut, "Prescila: A New, Lightweight Neutron Rem Meter," *Health Physics*  
456 **86** (2004) 603-612.  
457  
458 [18] J. Pope, *Radiat. Prot. Management* **11** (1994), 91-96.  
459  
460 [19] H. Toyokawa, A. Uritani, C. Mori, N. Takeda, K. Kudo, *IEEE Trans. Nuc. Sci.* **42** (1995)  
461 644.  
462  
463 [20] H. Toyokawa, A. Uritani, C. Mori, M. Yoshizawa, N. Takeda, K. Kudo, *Nuc. Inst. Meth.*  
464 *Phys. Res. A* **381** (1996) 481.  
465  
466 [21] H. Toyokawa, M. Yoshizawa, A. Uritani, C. Mori, N. Takeda, K. Kudo, *IEEE Trans.*  
467 *Nuc. Sci.* **44** (1997) 788.  
468  
469 [22] H. Toyokawa, A. Uritani, C. Mori, N. Takeda, K. Kudo, *Rad. Prot. Dos.* **70** (1997) 365.  
470  
471 [23] S. Yamaguchi, A. Uritani, H. Sakai, C. Mori, T. Iguchi, H. Toyokawa, N. Takeda, K.  
472 Kudo, *Nuc. Inst. Meth. Phys. Res. A* **422** (1999) 600.  
473  
474 [24] R.J. Sheu, J.S. Lin, S.H. Jiang, *Nuc. Inst. Meth. Phys. Res. A* **476** (2002) 74.  
475  
476 [25] J.L. Muniz, M.C. Vincente, E.M. Gonzalez, A.M. Romero, M. Embid, A. Delgado, *Rad.*  
477 *Prot. Dos.* **110** (2004) 243.  
478  
479 [26] Taosheng Li, Lianzhen Yang, Jizeng Ma, Dong Fang, *Rad. Prot. Dos.* **123** (2007) 15.  
480  
481 [27] Andrew C. Stephan and Vincent D. Jardret, *Neutron Detector*, United States Patent No.  
482 7,514,694 (2009).  
483  
484 [28] Stephen H. Manglos, *Neutron Range Spectrometer*, United States Patent No. 4,837,442  
485 (1989).  
486  
487 [29] Garry B. Spector, Tom McCollum, Alexander R. Spowart, *Nuc. Inst. Meth. Phys. Res. A*  
488 **346** (1994) 273.  
489  
490 [30] Y. Tanimura, J. Saegusa, M. Yoshizawa, M. Yoshida, *Nuc. Inst. Meth. Phys. Res. A* **547**  
491 (2005) 592.  
492

- 493 [31] Tom McCollum, *Scintillator Fiber Optic Long Counter*, United States Patent No.  
494 5,298,756 (1994).  
495
- 496 [32] D.T. Bartlett, R.J. Tanner, D.G. Jones, *Rad. Prot. Dos.* **74** (1997) 267.  
497
- 498 [33] M.J. Joyce, B.R. More, D.T. Bartlett, R.J. Tanner, D.G. Jones, *Neutron Radiation*  
499 *Detector*, United States Patent No. 6,362,485 (2002).  
500
- 501 [34] S.D. Monk, M.J. Joyce, *Rad. Prot. Dos.* **123** (2007) 3.  
502
- 503 [35] S.D. Monk, M.J. Joyce, Z. Jarrah, D. King, M. Oppenheim, *Rev. Sci. Inst.* **79** (2008)  
504 023301.  
505
- 506 [36] A.N. Caruso, *J. Phys.: Cond. Matt.* **22** (2010) 443201.  
507
- 508 [37] D.S. McGregor, W.J. McNeil, S.L. Bellinger, T.C. Unruh, J.K. Shultis, *Nuc. Inst. Meth.*  
509 *Phys. Res. A* **608** (2009) 125.  
510
- 511 [38] T.M. Oakes, "Modeling and Analysis of a Portable, Solid-State Neutron Detection  
512 System for Spectroscopic Applications", PhD Dissertation, 2012.  
513
- 514 [39] ICRP, *1990 Recommendations of the International Commission for Radiological*  
515 *Protection*, Publication 60, International Commission on Radiological Protection, *Annals*  
516 *of the ICRP*, **23**, Pergamon Press, Oxford, 1991.  
517
- 518 [40] Y. Xu, M. Flaska, S. Pozzi, V. Protopopescu, T. Downar, *Proc. of Joint Intl. Top. Meet.:*  
519 *M&C+SNA* (2007) Monterey, California.  
520
- 521 [41] A. Ferrari, M. Pelliccioni, *Rad. Prot. Dos.* **76** (1998) 215.  
522
- 523 [42] H. Schuhmacher, B. Siebert, *Rad. Prot. Dos.* **40** (1992) 85.  
524
- 525 [43] D. Bartlett, *Rad. Prot. Dos.* **15** (1986) 273.  
526
- 527 [44] B. Siebert, R. Hollnagel, *Rad. Prot. Dos.* **12** (1985) 145.  
528
- 529 [45] G. Leuthold, V. Mares, H. Schraube, *Rad. Prot. Dos.* **40** (1992) 77.  
530
- 531 [46] Y. Tanimura, J. Saegusa, M. Yoshizawa, M. Yoshida, *Nuc. Inst. Meth. Phys. Res. A* **346**  
532 (1994) 273-278.  
533
- 534 [47] Simon, Dan, "Optimal State Estimation: Kalman,  $H_\infty$ , and Nonlinear Approaches,"  
535 Hoboken, New Jersey: John Wiley & Sons, 2006.  
536



537 [48] IAEA, *Compendium of neutron spectra and detector responses for radiation protection*  
538 purposes. Technical Reports Series No. 403, Supplement to Technical Reports Series No.  
539 **318**. Vienna (2001).